Increased inducible nitric oxide synthase and arginase II expression in heart failure: no net nitrite/nitrate production and protein *S*-nitrosylation

Philipp Heusch, Stephanie Aker, Kerstin Boengler, Elisabeth Deindl, Anita van de Sand, Kristina Klein, Tienush Rassaf, Ina Konietzka, Adrian Sewell, Sara Menazza, Marcella Canton, Gerd Heusch, Fabio Di Lisa and Rainer Schulz

Am J Physiol Heart Circ Physiol 299:H446-H453, 2010. First published 28 May 2010;
doi:10.1152/ajpheart.01034.2009

You might find this additional info useful...

This article cites 66 articles, 39 of which can be accessed free at:
http://ajpheart.physiology.org/content/299/2/H446.full.html#ref-list-1

This article has been cited by 2 other HighWire hosted articles

C-Reactive Protein : Just a Biomarker of Inflammation or a Pathophysiological Player in Myocardial Function and Morphology?
Rainer Schulz and Gerd Heusch
Hypertension, February , 2011; 57 (2): 151-153.
[Full Text] [PDF]

A Radical View on the Contractile Machinery in Human Heart Failure
Gerd Heusch and Rainer Schulz
JACC, January 10, 2011; 57 (3): 310-312.
[Full Text] [PDF]

Updated information and services including high resolution figures, can be found at:
http://ajpheart.physiology.org/content/299/2/H446.full.html

Additional material and information about ***AJP - Heart and Circulatory Physiology*** can be found at:
http://www.the-aps.org/publications/ajpheart

This information is current as of April 9, 2012.

AJP - Heart and Circulatory Physiology publishes original investigations on the physiology of the heart, blood vessels, and lymphatics, including experimental and theoretical studies of cardiovascular function at all levels of organization ranging from the intact animal to the cellular, subcellular, and molecular levels. It is published 12 times a year (monthly) by the American Physiological Society, 9650 Rockville Pike, Bethesda MD 20814-3991. Copyright © 2010 by the American Physiological Society. ISSN: 0363-6135, ESSN: 1522-1539. Visit our website at http://www.the-aps.org/.

Downloaded from ajpheart.physiology.org on April 9, 2012

Am J Physiol Heart Circ Physiol 299: H446–H453, 2010.
First published May 28, 2010; doi:10.1152/ajpheart.01034.2009.

Increased inducible nitric oxide synthase and arginase II expression in heart failure: no net nitrite/nitrate production and protein *S*-nitrosylation

Philipp Heusch,[1] Stephanie Aker,[1] Kerstin Boengler,[1] Elisabeth Deindl,[2] Anita van de Sand,[1] Kristina Klein,[1] Tienush Rassaf,[3] Ina Konietzka,[1] Adrian Sewell,[4] Sara Menazza,[5] Marcella Canton,[5] Gerd Heusch,[1] Fabio Di Lisa,[5] and Rainer Schulz[1]

[1]*Institute for Pathophysiology, University of Essen Medical School, Essen;* [2]*Walter-Brendel-Centre of Experimental Medicine, University of Munich, Munich;* [3]*Department of Medicine, University of Düsseldorf, Düsseldorf; and* [4]*Department of Paediatrics, University Children's Hospital Frankfurt, Frankfurt, Germany; and* [5]*Department of Biomedical Sciences, University of Padova, Padova, Italy*

Submitted 2 November 2009; accepted in final form 25 April 2010

Heusch P, Aker S, Boengler K, Deindl E, van de Sand A, Klein K, Rassaf T, Konietzka I, Sewell A, Menazza S, Canton M, Heusch G, Di Lisa F, Schulz R. Increased inducible nitric oxide synthase and arginase II expression in heart failure: no net nitrite/nitrate production and protein *S*-nitrosylation. *Am J Physiol Heart Circ Physiol* 299: H446–H453, 2010. First published May 28, 2010; doi:10.1152/ajpheart.01034.2009.—Our objective was to address the balance of inducible nitric oxide (NO) synthase (iNOS) and arginase and their contribution to contractile dysfunction in heart failure (HF). Excessive NO formation is thought to contribute to contractile dysfunction; in macrophages, increased iNOS expression is associated with increased arginase expression, which competes with iNOS for arginine. With substrate limitation, iNOS may become uncoupled and produce reactive oxygen species (ROS). In rabbits, HF was induced by left ventricular (LV) pacing (400 beats/min) for 3 wk. iNOS mRNA [quantitative real-time PCR (qRT-PCR)] and protein expression (confocal microscopy) were detected, and arginase II expression was quantified with Western blot; serum arginine and myocardial nitrite and nitrate concentrations were determined by chemiluminescence, and protein *S*-nitrosylation with Western blot. Superoxide anions were quantified with dihydroethidine staining. HF rabbits had increased LV end-diastolic diameter [20.0 ± 0.5 (SE) vs. 17.2 ± 0.3 mm in sham] and decreased systolic fractional shortening (11.1 ± 1.4 vs. 30.6 ± 0.7% in sham; both $P < 0.05$). Myocardial iNOS mRNA and protein expression were increased, however, not associated with increased myocardial nitrite or nitrate concentrations or protein *S*-nitrosylation. The serum arginine concentration was decreased (124.3 ± 5.6 vs. 155.4 ± 12.0 μmol/l in sham; $P < 0.05$) at a time when cardiac arginase II expression was increased (0.06 ± 0.01 vs. 0.02 ± 0.01 arbitrary units in sham; $P < 0.05$). Inhibition of iNOS with 1400W attenuated superoxide anion formation and contractile dysfunction in failing hearts. Concomitant increases in iNOS and arginase expression result in unchanged NO species and protein *S*-nitrosylation; with substrate limitation, uncoupled iNOS produces superoxide anions and contributes to contractile dysfunction.

reactive oxygen species

THE INCIDENCE AND PREVALENCE of heart failure (HF) continue to increase (6, 40, 46), largely because patients survive myocardial infarction due to improved medical treatment (36). Apart from postmyocardial infarction remodeling, HF also results from hypertension (39), valvular disease (10), idiopathic cardiomyopathy or myocarditis (41), and occasionally tachycardia (45). Apart from the loss of cardiomyocytes (postmyocardial infarction or cardiomyocyte apoptosis), alterations in excitation-contraction coupling (34, 48) and oxidative modification of contractile myofilaments contribute to myocardial dysfunction (8, 9, 15, 28, 35).

Whereas inducible nitric oxide (NO) synthase (iNOS) is not detectable in normal cardiomyocytes, iNOS expression is increased in failing hearts in both animal models (2) and patients (18, 24, 58). Increased iNOS expression results from increased cardiomyocyte stretch secondary to protein kinase activation and, through positive feedback, from increased NO concentration (37).

NO mediates its effects either through cGMP and protein kinase G (52, 56) or more directly through protein nitrosylation (49). In the heart, NO reduces β-adrenergic responses (19, 22, 65), although that is controversial (50), and the L-type Ca-channel current (20), inhibits the mitochondrial respiratory chain (11, 14, 29, 32), and increases the mitochondrial permeability transition pore opening probability (53), thereby increasing cardiomyocyte apoptosis (3).

However, the contribution of increased iNOS expression to HF development has been questioned in transgenic mice with chronic cardiac-specific upregulation of iNOS (25, 44); only in the presence of a simultaneous knockout of myoglobin did iNOS overexpression result in HF (62).

In murine macrophages, increased iNOS expression is associated with a concomitant increase in arginase expression (59). Recent data from wound healing studies in rats suggest that there might be a self-limiting negative feedback cycle, in that increased iNOS-derived NO increases arginase II activity, which subsequently reduces L-arginine concentration and thereby limits NO production (66). Limitation of substrate availability also leads to uncoupling of iNOS with ultimate reactive oxygen species (ROS) formation (49, 60). Increased ROS formation induces myofibrillar oxidation and subsequently contributes to the development of contractile dysfunction (8, 9). An interaction between iNOS and arginase has not yet been studied in the failing heart.

We have now used our established model of pacing-induced HF in rabbits to assess both iNOS and arginase protein expression in normal and failing hearts. It is particularly the arginase II isoform that is expressed in cardiomyocyte mitochondria (57). Also, we assessed neuronal NOS (nNOS) mRNA and protein expression, NO and superoxide anion formation, as well as protein *S*-nitrosylation along with contractile function in failing rabbit hearts. To address the functional importance of increased iNOS expression and its contribu-

Address for reprint requests and other correspondence: R. Schulz, Institute for Pathophysiology, Univ. of Essen Medical School, Hufelandstraße 55, 45122 Essen, Germany (e-mail: rainer.schulz@uk-essen.de).

0363-6135/10 Copyright © 2010 the American Physiological Society

Downloaded from ajpheart.physiology.org on April 9, 2012

tion to superoxide anion formation, iNOS inhibition was achieved with 1400W (21).

METHODS

The present study was approved by the bioethical committee of the district of Düsseldorf, Germany, and the investigation conforms with the Guide for the Care and Use of Laboratory Animals published by the National Institutes of Health (NIH publication no. 85-23, revised 1996).

Experimental model and protocols. Male Chinchilla bastard rabbits (Charles River, Kisslegg, Germany) received a standard chow (ssniff, Soest, Germany) that contained nitrate, but this chow was the same for all experimental groups. Rabbits with an age of 18–20 wk weighing 3–4 kg were anesthetized, initially with ketamine (50 mg/kg)-xylazine (3 mg/kg) and subsequently with propofol (12–25 ml/h)-fentanyl (0.003 mg/kg), intubated, and ventilated using a Dräger UV-2 ventilator (Lübeck, Germany) with 70% room air and 30% oxygen. After a left thoracotomy, a pacing lead was sutured onto the apical region of the left ventricle (LV). The pacing lead was connected to a pacemaker (Medtronic, Düsseldorf, Germany), which was implanted subcutaneously. The chest was closed in layers and evacuated with a Bülau drainage. The tracheal tube was removed after spontaneous breathing was assured. The rabbits were placed on an antibiotic regimen (12 mg/kg enrofloxacin) for 3 days, and postoperative analgesia was achieved with buprenorphin (0.03 mg/kg). After instrumentation, the rabbits were allowed to recover for 7–10 days.

Development of HF. HF was induced by rapid LV pacing (400 beats/min) for 1 (HF1; $n = 7$), 2 (HF2; $n = 7$), or 3 wk (HF3; $n = 6$), respectively. HF was evident from clinical signs, such as ascites and cachexia, and echocardiographic parameters, such as a reduction of LV systolic fractional shortening (LVS-FS) and an increase in LV end-diastolic diameter (LVEDD). Ten sham rabbits underwent surgery and were followed for the same 3-wk time frame as HF rabbits. Echocardiography was performed on a weekly basis. There was no change in any measured parameter throughout the observation period, and data after 3 wk are presented in sham rabbits.

iNOS inhibition with 1400W. Seven rabbits received the iNOS inhibitor 1400W (1 $mg \cdot kg^{-1} \cdot day^{-1}$ sc) at the onset of pacing, and 6 rabbits received placebo. Higher concentrations of 1400W ($\leq$5 $mg \cdot kg^{-1} \cdot day^{-1}$) over 3 wk induced gastrointestinal hemorrhage and necrosis even in sham rabbits. Sixteen sham rabbits served as controls, eight each with 1400W or placebo.

After euthanasia of the rabbits, 4–6 samples (50 mg each) were taken from the LV free wall; 2–3 samples each were frozen in liquid nitrogen and stored at −70°C until further use or were fixed in formalin and embedded in paraffin.

Echocardiography. LV function (Supervision 7000; Toshiba, Neuss, Germany) was measured in the short-axis view at baseline and after 1, 2, and 3 wk of pacing while the rabbits were conscious and the pacemaker had been turned off for at least 60 min. LVS-FS was calculated from LVEDD and end-systolic diameter [(LVEDD − end-systolic diameter)/LVEDD × 100]. End-diastole and end-systole were determined from the electrocardiogram (55).

Histology. Apoptosis was determined using the TdT-mediated dUTP nick end labeling (TUNEL) technique (In Situ Cell Death Detection Kit; La Roche Diagnostics, Mannheim, Germany), counterstaining with bisbenzimide (HOE-33342) and phalloidin (both Sigma, Taufkirchen, Germany). TUNEL-positive cardiomyocyte nuclei were counted using fluorescence microscopy (Leica DM LB, Bensheim, Germany) and calculated per square millimeter. The extent of myocardial fibrosis was determined by Masson-Goldner trichrome staining and expressed as percentage of field of view (3 fields of 0.075 mm^2 each) (55).

Quantitative real-time PCR. Total RNA was isolated according to the procedure of Chomczynski and Sacchi (12) from frozen heart samples isolated from sham-operated rabbits ($n = 5$) or rabbits undergoing 3 wk of pacing ($n = 6$). One microgram of DNase-treated total RNA was reverse-transcribed using random nonamers (La Roche Diagnostics) and a 1st Strand cDNA Synthesis Kit for RT-PCR (La Roche Diagnostics). Quantitative real-time PCR (qRT-PCR) was performed with a Light Cycler 1.5 (La Roche Diagnostics) in a reaction volume of 10 μl using a Light Cycler FastStart DNA Master^{Plus} SYBR Green I Kit (La Roche Diagnostics) and 50 pmol of each primer (nNOS, forward: 5′-GCC AAG GTG ATG TCC ATG-3′; reverse: 5′-GTG CCT CAT TTC CAT CAA G-3′; iNOS, forward: 5′-CAG AGC AGT ACA AGC TCA C-3′; reverse: 5′-GGA TCT CAG CCT CAT GGT G-3′; 18S, forward: 5′-GGA CAG GAT TGA CAG ATT GAT AG-3′; reverse: 5′-CTC GTT CGT TAT CGG AAT TAA C-3′). At least two independent qRT-PCR reactions were performed on each template. The protocol was as follows: an initial denaturation step at 95°C for 10 min was followed by 50 cycles of denaturation (95°C, 10 s), annealing (56°C for nNOS, 60°C for iNOS, 64°C for 18S rRNA, 5 s), and extension (72°C, 15 s). Melt curve analyses were performed to control specific amplification. Results were normalized to the expression levels of the 18S rRNA.

Confocal laser scan microscopy of iNOS and arginase II. Frozen biopsies were embedded in optimum cutting temperature (OCT) Cryomatrix embedding medium (Shandon, Pittsburgh, PA), and sections of 5 μm were cut in a cryostat. Cryomatrix was removed with PBS. The primary mouse anti-mouse iNOS antibody (dilution 1:10; Transduction Laboratories, Lexington, KY) or the primary goat anti-human arginase II antibody (dilution 1:20; sc-18357; Santa Cruz Biotechnology) was applied, and sections were incubated for 2 h at 37°C. Several rinsing steps with PBS followed, and a FITC-conjugated secondary goat anti-mouse $IgG_{2\alpha}$ antibody (sc-2079; Santa Cruz Biotechnology) or secondary donkey anti-goat (sc-2024; Santa Cruz Biotechnology) was applied for 1 h at 37°C. Negative controls were identical except for the lack of primary antibodies. The samples were coverslipped in Vectashield (H-1000; Vector Laboratories, Burlingame, CA) and examined by laser scan microscopy (LSM Pascal 5; Zeiss, Jena, Germany) at ×400 magnification for iNOS and at ×630 magnification for arginase II. For analysis of both iNOS and arginase II, images of 4 fields of view (0.053 mm^2 each) at an optimal focus were taken. The density of FITC immunofluorescence in the entire area was analyzed and expressed in arbitrary units (AU). To eliminate background staining, AU values from negative control tissue samples were subtracted.

Western blot analysis. Tissue samples were homogenized in 1× cell lysis buffer (containing 20 mM Tris, pH 7.5, 150 mM NaCl, 1 mM EDTA, 1 mM EGTA, 2.5 mM sodium pyrophosphate, 1 mM β-glycerolphosphate, 1 mM Na_3VO_4, 1% Triton X-100, 1 μg/ml leupeptin; Cell Signaling, Danvers, MA), supplemented with 1× Complete Protease Inhibitor Cocktail (La Roche Diagnostics). After sonication, the samples were centrifuged at 14,000 *g* for 10 min at 4°C. The protein concentration of the supernatant was determined using the DC Protein Assay Kit (Bio-Rad, Hercules, CA). Thirty micrograms of total protein were electrophoresed on 10% Bis-Tris gels (Bio-Rad) and transferred to nitrocellulose membranes (Bio-Rad). After blocking, the membranes were incubated overnight at 4°C with goat polyclonal IgG antibodies against human arginase II (dilution 1:200; sc-18357; Santa Cruz Biotechnology) or with rabbit polyclonal IgG antibodies against rat nNOS (dilution 1:200; Invitrogen, Carlsbad, CA). After incubation with the respective secondary antibodies, immunoreactivities were detected using the SuperSignal West Femto Maximum Sensitivity Substrate (Pierce, Rockford, IL). Signal intensities were quantified using the Scion Image software (Frederick, MD).

Since antibodies are not always specific (31), Western blot analysis for arginase II was performed on protein extracts isolated from the kidneys of wild-type and arginase II knockout mice and from the kidneys and LV of rabbits. Arginase II immunoreactivity was found in rabbit LV protein extracts, in rabbit and wild-type mouse kidneys, but not in the kidney of arginase II knockout mice, demonstrating the specificity of the anti-arginase II antibody used.

Downloaded from ajpheart.physiology.org on April 9, 2012

Immunoprecipitation. For immunoprecipitation, 400-μg proteins extracted from the LV of sham rabbits were incubated with rabbit anti-nNOS or anti-rabbit horseradish peroxidase-conjugated IgGs for 1 h at 4°C. Protein A/G PLUS-Agarose (Santa Cruz Biotechnology) was added to each sample followed by overnight incubation at 4°C. The Protein A/G PLUS-Agarose beads were washed three times with 500 μl of 1× PBS supplemented with protease inhibitors. After adding sample buffer, the samples were boiled, and the supernatants were subjected to Western blot analysis.

Serum L-arginine concentration. Serum samples for the determination of free L-arginine were deproteinized with sulphosalicylic acid and centrifuged, and the supernatants were subjected to automated ion-exchange chromatography with postcolumn ninhydrin detection (Biochrom 30 Amino Acid Analyzer).

Tissue nitrite/nitrate concentrations. For determination of the nitrite/nitrate concentrations, tissue was kept on ice and homogenized in a 1:5 ratio with *N*-ethylmaleimide (NEM)-EDTA solution (100 mM NEM, 2.5 mM EDTA in 0.9% NaCl solution). The homogenate was then split into two fractions. The first fraction, which was used for the measurement of nitrite, was not treated further but injected directly. The first fraction comprises nitrite, nitrate, and all nitrosylated proteins, but after substration of nitrate (second fraction) it is made up by >95% of nitrite (7) and was therefore considered as nitrite in the present study. The second fraction was used to determine nitrate and was first deproteinized with methanol in a 1:2 ratio. After centrifugation at 14,000 *g* for 15 min, nitrate reductase (0.1 IU/ml), glucose-6-phosphate (1 mM), NADPH (2 mM), and glucose-6-phosphate dehydrogenase (0.3 IU/ml) were added to the supernatant for the conversion of nitrate to nitrite. The suspension was incubated for 1 h at 25°C in the dark before measurement. Through chemiluminescence detection (CLD 88NOe; ECO Physics, Dürnten, Switzerland), both samples were then determined after reductive cleavage by an iodide/triiodide-containing reaction mixture. The subsequent NO release into the gas phase was measured by its chemiluminescence reaction with ozone (O_3) (27).

Protein S-nitrosylation. The occurrence of protein *S*-nitrosylation in LV biopsies was assessed by means of the biotin switch assay (30) on Protein Detection Kit (Cayman Chemical). This method is aimed at converting nitrosylated cysteines into biotinylated cysteines in a three-step procedure. Briefly, the tissue samples were homogenized in ice-cold PBS, pH 7.2, containing 1 mM EDTA and 0.1 mM neocuproine, and centrifuged at 12,000 *g* for 5 min at 4°C. The resulting pellet underwent the biotin switch assay. In the first step, protein-free thiols were blocked by incubation with the thiol-specific agent methyl methanethiosulfonate. In the second step, *S*-nitrosothiols were selectively reduced by ascorbate to form thiols, which were then reacted with *N*-[6-(biotinamido)hexyl]-3′-(2′-pyridyldithio) propionamide, a sulfhydryl-specific biotinylating reagent. Both preparative procedures were performed in the dark to prevent light-induced cleavage of *S*-nitrosylated proteins. Then, the biotinylated/*S*-nitrosylated proteins were subjected to immunoblot analysis with anti-biotin antibodies. Densitometry was performed on scanned immunoblots using the ImageJ computer program (NIH, Bethesda, MD). The biotin switch assay measures only *S*-nitrosylation and not *N*-nitrosylation, which in the rat heart is of equal magnitude (7).

Superoxide anion concentration. The production of superoxide anions was detected by DHE (D-11347; Molecular Probes, Eugene, OR), a fluorescent dye. In the presence of superoxide, it is oxidized to ethidium bromide, which is excited at 488 nm with an emission spectrum of 610 nm. Frozen tissue samples were embedded in OCT (Cryomatrix) and cut into 10-μm sections at −20°C. Sections were mounted on glass slides. DHE at a solution of 2 μM was applied and incubated at 37°C for 30 min in a humidified chamber. To assure a blockade of iNOS by 1400W, we also added 1400W ex vivo (2 μM) as a control. Negative controls were obtained by blocking the reaction with 100 mM *N*-acetyl-L-cysteine (NAC; A9165; Sigma) for 30 min before DHE staining. Four images were taken with a laser scanning microscope (LSM Pascal 5; Zeiss, Oberkochen, Germany) including a krypton/argon laser. Three fields of 0.075 mm^2 each were analyzed.

Statistics. Data are expressed as mean values ± SE. Heart rate, LVS-SF, LVEDD, iNOS and arginase II expression and serum arginine concentration in sham rabbits and HF rabbits after 1, 2, and 3 wk of LV pacing were compared by one-way-ANOVA. Each time point is represented by separate animals that had to be killed at that time point for tissue sampling. When there was a significant overall effect, individual mean values were compared using Bonferroni method. Tissue nitrite, nitrate, protein *S*-nitrosylation, NOS mRNA and protein data, and superoxide anion data of sham rabbits and HF rabbits after 3 wk of LV pacing were compared by unpaired Student's *t*-test. Heart rate, LV function, LV histology, and superoxide anion data in shams and HF rabbits after 3 wk of pacing, each after placebo or inhibition of iNOS with 1400W, were compared using a two-way-ANOVA, again with post hoc comparison of single mean values using Bonferroni method. All statistics were performed using the SigmaStat program. A P value <0.05 was considered significant.

RESULTS

Ventricular function. In rabbits with rapid LV pacing, LVEDD increased, whereas LVS-FS decreased with the progression of HF (Table 1). Heart rate was increased in HF, albeit significantly only in HF-1 and HF-2.

NOS and arginase II expression, serum arginine concentration, tissue nitrite/nitrate concentrations, and protein S-nitrosylation. Using confocal microscopy, myocardial iNOS expression increased by 8.6 ± 0.4-fold only after 3 wk of pacing (HF-3 vs. sham; Fig. 1). Using qRT-PCR, only in three out of six sham rabbits SYBR Green fluorescence reached a value above the background fluorescence indicating iNOS amplification. However, the threshold cycle >43 suggested only marginal amounts of iNOS mRNA in LV tissue of sham rabbits. In contrast, iNOS amplification was detected in six out of six HF-3 rabbits with threshold cycles ranging from 39 to 43, also suggesting increased amounts of iNOS mRNA in HF-3 compared with sham rabbits. The increased iNOS expression was not associated with an increase in the myocardial nitrite or nitrate concentrations (Table 2) or protein *S*-nitrosylation (Fig. 2). Arginase II expression increased continuously up to threefold with the progression of HF (Fig. 3), whereas serum L-arginine concentration decreased (Table 2). The increase of arginase II expression was confirmed by confocal laser scan microscopy (data not shown). Also, the nNOS mRNA (normalized to 18S rRNA) was significantly decreased in HF-3 (0.79 ± 0.08 AU, $n = 6$) compared with sham rabbits (1.82 ± 0.13 AU, $n = 5$). The results of the qRT-PCR were confirmed by Western blot analysis (nNOS normalized to Ponceau: 0.06 ± 0.02 AU in

Table 1. *Heart rate and left ventricular function during the progression of heart failure*

	Sham	HF1	HF2	HF3
Heart rate, beats/min	226 ± 10	258 ± 9*	279 ± 9*	254 ± 11
LVS-FS, %	30.6 ± 0.7	19.2 ± 0.6*	16.7 ± 1.0*†	11.1 ± 1.4*†‡
LVEDD, mm	17.2 ± 0.3	18.6 ± 0.4	19.3 ± 0.3*	20.0 ± 0.5*†

Values are means ± SE. Sham, sham-operated rabbits ($n = 8$); HF1, heart failure (HF) rabbits, 1-wk pacing ($n = 8$); HF2, HF rabbits, 2-wk pacing ($n = 8$); HF3, HF rabbits, 3-wk pacing ($n = 7$); LVS-FS, left ventricular (LV) systolic fractional shortening; LVEDD, LV end-diastolic diameter. *$P < 0.05$ vs. Sham; †$P < 0.05$ vs. HF1; ‡$P < 0.05$ vs. HF2.

Downloaded from ajpheart.physiology.org on April 9, 2012

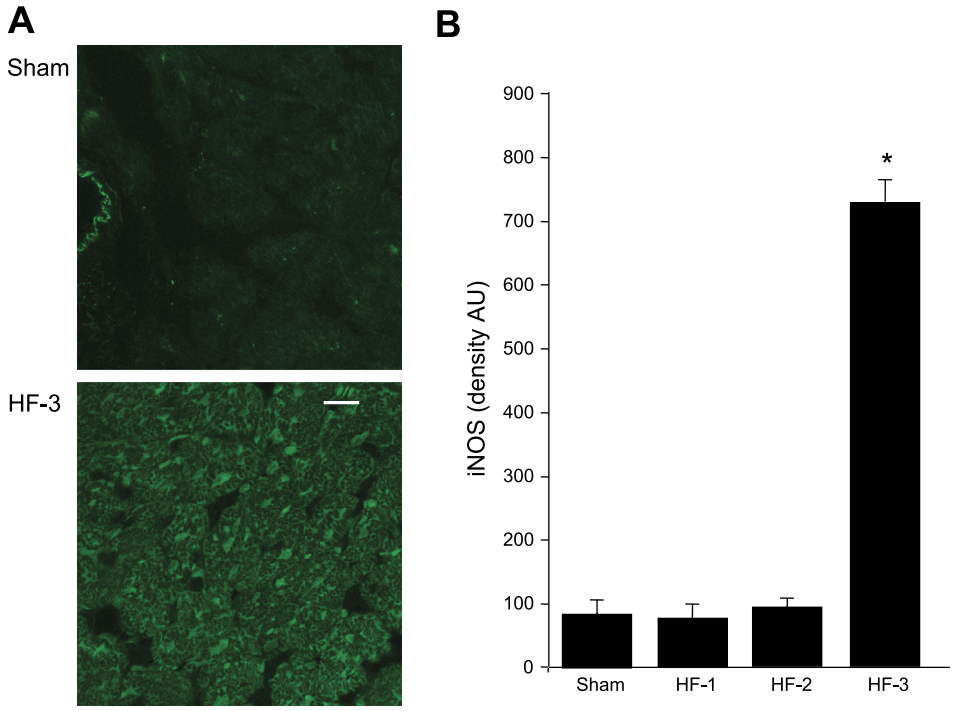

Fig. 1. *A*: confocal laser scan microscopy of inducible nitric oxide (NO) synthase (iNOS) in myocardial rabbit tissue at ×400 magnification. Sham, sham-operated rabbits; HF3, heart failure rabbits, 3-wk pacing. Scale bar = 50 μm. *B*: myocardial iNOS expression increases during the time course of 3-wk rapid left ventricular (LV) pacing compared with shams. Data are expressed as means ± SE. *$P < 0.05$ vs. Sham. Sham, sham-operated rabbits (n = 8); HF1, heart failure rabbits, 1-wk pacing (n = 8); HF2, heart failure rabbits, 2-wk pacing (n = 8); HF3, heart failure rabbits, 3-wk pacing (n = 7); AU, arbitrary units.

HF-3 vs. 0.02 ± 0.01 in sham rabbits; $P < 0.05$). No protein-protein interaction between arginase II and nNOS was detected by coimmunoprecipitation.

iNOS inhibition. There was no difference in heart rate, LVEDD, LVS-FS, TUNEL-positive cardiomyocytes, or the extent of fibrosis between sham rabbits without or with 1400W. In HF rabbits with placebo, LVEDD increased and LVS-FS decreased after 3 wk of LV pacing, along with increased ROS formation, TUNEL-positive cardiomyocytes, and the extent of fibrosis (Table 3). In HF rabbits treated with 1400W, LVS-FS after 3 wk of pacing was better preserved than in HF rabbits with placebo (Table 3). The increased ROS formation in failing myocardium was attenuated by iNOS blockade in vivo (Table 3) and ex vivo (860 ± 60 AU in HF vs. 683 ± 19 AU in HF with 1400W; $P < 0.05$). Also, the number of TUNEL-positive cardiomyocytes and the extent of fibrosis were reduced by 1400W.

DISCUSSION

We found no evidence for increased NO-related species and protein *S*-nitrosylation in our pacing-induced HF model despite an increased expression of iNOS. Inhibition of iNOS in the presence of limited substrate, possibly secondary to increased arginase II expression in failing hearts, reduced ROS formation and attenuated LV contractile dysfunction.

Limitations. All animals received the same diet without any supplementation of L-arginine or cofactors of NOS to compensate for any potential decline occurring during HF develop-

Table 2. *Tissue nitrite, nitrate, and serum arginine concentrations and cardiac protein S-nitrosylation as well as ROS concentration in sham and HF rabbits after 3 wk of pacing*

	Sham	HF3
Nitrite, μM	2.41 ± 0.58	1.98 ± 0.54
Nitrate, μM	13.9 ± 2.9	9.5 ± 0.6
Arginine, μmol/l	155.4 ± 12.0	124.3 ± 5.6*
Protein *S*-nitrosylation, AU	94.0 ± 5.7	103.0 ± 22.0
ROS, AU	546 ± 20	860 ± 60*

Values are means ± SE. Sham, n = 8; HF3, n = 7; ROS, reactive oxygen species; AU, arbitrary units. *$P < 0.05$ vs. Sham. Data from sham rabbits are after 3 wk.

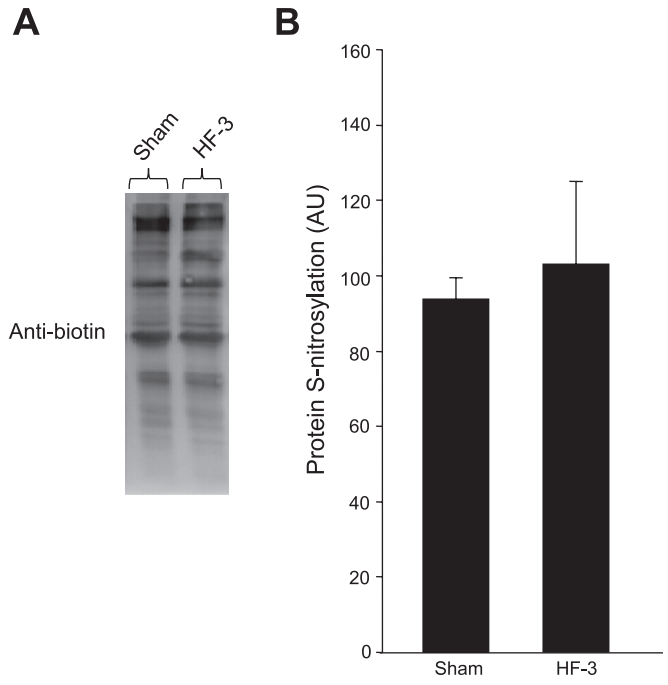

Fig. 2. *A*: representative immunoblot stained with anti-biotin antibodies in sham rabbits and heart failing rabbits after 3 wk of rapid LV pacing. *B*: protein *S*-nitrosylation did not increase after 3 wk of rapid LV pacing compared with shams. Data are expressed as means ± SE. Sham, n = 8; HF3, n = 7.

Downloaded from ajpheart.physiology.org on April 9, 2012

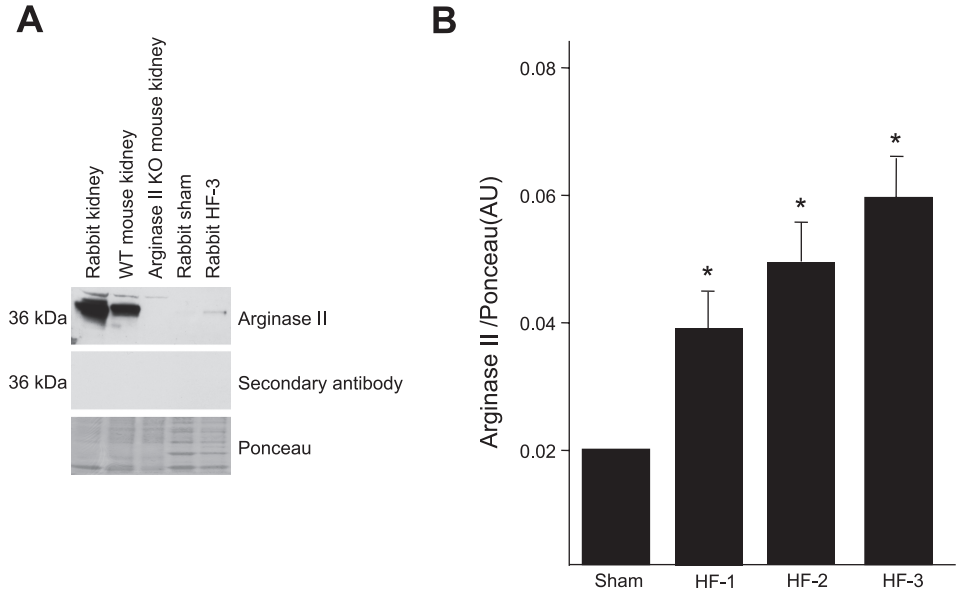

Fig. 3. *A*: representative Western blot of arginase II in sham rabbits ($n = 6$) and heart failure rabbits after 3 wk of rapid LV pacing ($n = 6$). *B*: arginase II expression increases during the time course of 3-wk rapid LV pacing compared with shams. Data are expressed as means ± SE. *$P < 0.05$ vs. Sham. Sham, $n = 8$; HF1, $n = 8$; HF2, $n = 8$; HF3, $n = 7$; WT, wild-type; KO, knockout.

ment. Supplementation of L-arginine and/or essential cofactors could have altered the results of the present study by preventing a potential uncoupling of iNOS and thus leading to higher amounts of NO.

The results of the qRT-PCR suggest increased amounts of iNOS mRNA in HF-3 compared with sham rabbits. However, the overall low iNOS content did not permit the accurate quantification of iNOS mRNA. Although we were able to detect the low iNOS protein content in tissue sections using confocal microscopy, we could not quantify iNOS protein in LV tissue homogenates of sham or HF-3 rabbits using Western blot analysis. A 10-fold higher sensitivity for protein detection by confocal microscopy than by Western blot analysis (5) and the detection of a low-abundance myocardial protein, such as connexin45, by confocal microscopy but not by Western blot analysis have been demonstrated before (13). NOS activity assays were not performed in the present study.

Protein *S*-nitrosylation, which was unaltered in failing hearts, is mediated by peroxynitrite formation (16, 17). Therefore, to confirm the above data, measurements of tissue peroxynitrite levels would have been useful, however, were not performed in the present study.

We did not measure blood pressure in placebo and 1400W-treated animals. There have been several reports on iNOS blockade with 1400W and blood pressure responses in short-term and long-term animal models (4, 23, 33, 51, 54, 64). In most studies, except for those on endotoxin shock, 1400W at concentrations far above the one used in the present study (>5 mg/kg) for durations of up to 2 wk (64) did not affect blood pressure. In endotoxin shock (51, 54), however, 1400W maintained blood pressure by attenuating excessive NO formation. Since NO formation did not increase in the present study despite an increased iNOS expression, it appears unlikely that 1400W increased blood pressure and afterload and thereby affected LVS-FS to any significant extent.

We used our established pacing-induced HF model in rabbits. Tachycardia is only rarely the cause of HF in humans (45). Nevertheless, pacing-induced HF is an established and reproducible experimental model of global, homogeneous, relatively quickly developing and then stable LV contractile dysfunction (42, 43, 47). The pacing-induced HF model in rabbits is characterized by typical clinical signs of ascites, cachexia, and splanchnic congestion (1), typical morphological features such as cardiomyocyte hypertrophy, cardiomyocyte apoptosis, and increased fibrosis (2, 55), typical autonomic changes such as increased plasma catecholamines and subsequent β-adrenoceptor downregulation, and enhanced systemic tumor necrosis factor-α concentrations (1).

NOS and arginase II expression. Using different methodologies to measure tissue nitrite/nitrate concentrations and protein *S*-nitrosylation, no evidence for enhanced myocardial NO-related species or NO-mediated effects were detected in

Table 3. *Heart rate, LV function, ROS concentration, and iNOS expression in sham and HF rabbits without and with inhibition of iNOS with 1400W*

	Sham	Sham 1400W	HF	HF 1400W
Heart rate, beats/min	226 ± 10	224 ± 5	254 ± 11*	261 ± 8
LVS-FS, %	30.6 ± 0.7	30.1 ± 0.6	11.1 ± 1.4*	15.1 ± 1.6†
LVEDD, mm	17.2 ± 0.3	17.0 ± 0.5	20.0 ± 0.5*	19.0 ± 0.3
TUNEL, /1,000 × mm^2	0.015 ± 0.005	0.015 ± 0.004	0.062 ± 0.008*	0.045 ± 0.014*†
Extent of fibrosis, %	5.9 ± 0.4	6.3 ± 0.3	14.1 ± 1.4	10.6 ± 0.5*†
ROS, AU	546 ± 20	473 ± 34	860 ± 60*	705 ± 24.4†

Values are means ± SE. iNOS, inducible nitric oxide synthase; Sham, $n = 8$; Sham 1400W, sham-operated rabbits treated with 1400W; HF3, $n = 7$; TUNEL, TdT-mediated dUTP nick end labeling (TUNEL)-positive cardiomyocytes. *$P < 0.05$ vs. Sham; †$P < 0.05$ vs. HF.

Downloaded from ajpheart.physiology.org on April 9, 2012

failing hearts. We observed increases in the expression of both iNOS and arginase II, but increased expression of arginase II preceded that of iNOS. The increase of iNOS expression after only 3 wk of LV pacing is consistent with increased phosphorylation of p38 MAPK at that time (2, 55), and p38 MAPK is an upstream signal of iNOS (2). In the present study, increased iNOS expression was probably not stretch-induced because LVEDD increased already after 2 wk of pacing, whereas iNOS expression was induced only after 3 wk of rapid LV pacing.

It is unclear which signal increased the expression of arginase II in failing hearts, but in murine macrophages arginase II protein expression is increased by p38 MAPK and ERK activation (38). In failing hearts, p38 MAPK is unlikely to be an upstream signal of arginase II because p38 MAPK is increased only after 3 wk of rapid LV pacing (55), whereas arginase II expression was increased already after 1 wk of pacing. In support of this, after blockade of p38 MAPK, a similar increase of arginase II expression was measured after 3 wk of rapid LV pacing (data not shown).

NOS and superoxide anion formation. Increased iNOS expression in the presence of limited substrate might result in uncoupling of iNOS (49, 60), thus potentially promoting ROS formation and oxidative modification of myofilaments and ultimately contributing to contractile failure (8, 9). Indeed iNOS inhibition with 1400W attenuated superoxide anion formation and LV contractile dysfunction. In contrast, iNOS overexpression in a transgenic mice model did not impact on LV contractile function (25). In this model, iNOS was functionally coupled (as indicated by the citrulline assay) and resulted in high concentrations of nitrate. Only in the presence of a simultaneous knockout of myoglobin, thereby avoiding nitrate formation, iNOS overexpression resulted in contractile dysfunction (62). Thus functionally coupled iNOS does not contribute to contractile failure as long as NO is rapidly processed to nitrate.

Our results characterize only the pacing-induced HF model in the strictest sense. We cannot exclude that in HF of different origin (e.g., inflammation or genetic cardiomyopathy) or as the consequence of a more regional event (e.g., myocardial infarction), the increase in iNOS expression may impact on LV contractile function. Of note, in a pig model of short-term hibernation, iNOS expression and NO formation were increased after only 6 h and had an impact on cardiomyocyte function (26).

Further studies are warranted to look at potential dietary interventions and, of note, to look at potential arginase upregulation in biopsy samples from human failing hearts.

Significance and perspectives. An increase in iNOS expression does not necessarily imply increased NO-induced myocardial damage; nevertheless, uncoupled iNOS secondary to substrate limitation might contribute to contractile dysfunction through increased oxidative stress. Increased arginase expression might limit NOS substrate availability and contribute to the persistence of hypertension (61, 63). Whether increased arginase expression also contributes to the development/progression of HF by promoting iNOS uncoupling warrants further investigation. Certainly, blockade of enhanced arginase expression/activity might be a promising new therapeutic approach since iNOS, as long as it is functionally coupled, does not contribute to HF development (25).

ACKNOWLEDGMENTS

We thank Mei-Ping Wu for technical assistance in generating the qRT-PCR data. This paper reports the Doctor of Medicine thesis of P. Heusch.

GRANTS

The study was supported by a grant form the German Research Foundation, Bonn, Germany (BR526/12-1).

DISCLOSURES

No conflicts of interest, financial or otherwise, are declared by the author(s).

REFERENCES

1. **Aker S, Belosjorow S, Konietzka I, Duschin A, Martin C, Heusch G, Schulz R.** Serum but not myocardial TNF-α concentration is increased in pacing-induced heart failure in rabbits. *Am J Physiol Regul Integr Comp Physiol* 285: R463–R469, 2003.
2. **Aker S, Snabaitis AK, Konietzka I, van de Sand A, Böngler K, Avkiran M, Heusch G, Schulz R.** Inhibition of the Na^+/H^+ exchanger attenuates the deterioration of ventricular function during pacing-induced heart failure in rabbits. *Cardiovasc Res* 63: 273–282, 2004.
3. **Andreka P, Tran T, Webster KA, Bishopric NH.** Nitric oxide and promotion of cardiac myocyte apoptosis. *Mol Cell Biochem* 263: 35–53, 2004.
4. **Bagnall NM, Dent PC, Walkowska A, Sadowski J, Johns EJ.** Nitric oxide inhibition and the impact on renal nerve-mediated antinatriuresis and antidiuresis in the anaesthetized rat. *J Physiol* 569: 849–856, 2005.
5. **Bieschke J, Giese A, Schulz-Schaeffer W, Zerr I, Poser S, Eigen M, Kretzschmar H.** Ultrasensitive detection of pathological prion protein aggregates by dual-color scanning for intensely fluorescent targets. *Proc Natl Acad Sci USA* 97: 5468–5473, 2000.
6. **Bleumink GS, Knetsch AM, Sturkenboom MC, Straus SM, Hofman A, Deckers JW, Witteman JC, Stricker BH.** Quantifying the heart failure epidemic: prevalence, incidence rate, lifetime risk and prognosis of heart failure. The Rotterdam Study. *Eur Heart J* 25: 1614–1619, 2004.
7. **Bryan NS, Rassaf T, Maloney RE, Rodriguez CM, Saijo F, Rodriguez JR, Feelisch M.** Cellular targets and mechanisms of nitros(yl)ation: an insight into their nature and kinetics in vivo. *Proc Natl Acad Sci USA* 101: 4308–4313, 2004.
8. **Canton M, Neverova I, Menabò R, Van Eyk J, Di Lisa F.** Evidence of myofibrillar protein oxidation induced by postischemic reperfusion in isolated rat hearts. *Am J Physiol Heart Circ Physiol* 286: H870–H877, 2004.
9. **Canton M, Skyschally A, Menabo R, Boengler K, Gres P, Schulz R, Haude M, Erbel R, Di Lisa F, Heusch G.** Oxidative modification of tropomyosin and myocardial dysfunction following coronary microembolization. *Eur Heart J* 27: 875–881, 2006.
10. **Carabello BA.** Aortic stenosis: from pressure overload to heart failure. *Heart Fail Clin* 2: 435–442, 2006.
11. **Chen Y, Traverse JH, Du R, Hou M, Bache RJ.** Nitric oxide modulates myocardial oxygen consumption in the failing heart. *Circulation* 106: 273–279, 2002.
12. **Chomczynski P, Sacchi N.** Single-step method of RNA isolation by acid guanidinium thiocyanate-phenol-chloroform extraction. *Anal Biochem* 162: 156–159, 1987.
13. **Coppen SR, DuPont E, Rothery S, Severs NJ.** Connexin45 expression is preferentially associated with the ventricular conduction system in mouse and rat heart. *Circ Res* 82: 232–243, 1998.
14. **Davidson SM, Duchen MR.** Effects of NO on mitochondrial function in cardiomyocytes: pathophysiological relevance. *Cardiovasc Res* 71: 10–21, 2006.
15. **de Tombe PP, Solaro RJ.** Integration of cardiac myofilament activity and regulation with pathways signaling hypertrophy and failure. *Ann Biomed Eng* 28: 991–1001, 2000.
16. **Ferdinandy P.** Peroxynitrite: just an oxidative/nitrosative stressor or a physiological regulator as well? *Br J Pharmacol* 148: 1–3, 2006.
17. **Ferdinandy P, Schulz R.** Nitric oxide, superoxide, and peroxynitrite in myocardial ischaemia-reperfusion injury and preconditioning. *Br J Pharmacol* 138: 532–543, 2003.
18. **Fukuchi M, Hussain SN, Giaid A.** Heterogeneous expression and activity of endothelial and inducible nitric oxide synthases in end-stage human heart failure: their relation to lesion site and β-adrenergic receptor therapy. *Circulation* 98: 132–139, 1998.

Downloaded from ajpheart.physiology.org on April 9, 2012

19. **Funakoshi H, Kubota T, Kawamura N, Machida Y, Feldman AM, Tsutsui H, Shimokawa H, Takeshita A.** Disruption of inducible nitric oxide synthase improves β-adrenergic inotropic responsiveness but not the survival of mice with cytokine-induced cardiomyopathy. *Circ Res* 90: 959–965, 2002.
20. **Gallo MP, Malan D, Bedendi I, Biasin C, Alloatti G, Levi RC.** Regulation of cardiac calcium current by NO and cGMP-modulating agents. *Pflügers Arch* 441: 621–628, 2001.
21. **Garvey EP, Oplinger JA, Furfine ES, Kiff RJ, Laszlo F, Whittle BJ, Knowles RG.** 1400 W is a slow, tight binding, and highly selective inhibitor of inducible nitric oxide synthase in vitro and in vivo. *J Biol Chem* 272: 4959–4963, 1997.
22. **Gealekman O, Abassi Z, Rubinstein I, Winaver J, Binah O.** Role of myocardial inducible nitric oxide synthase in contractile dysfunction and β-adrenergic hyporesponsiveness in rats with experimental volume-overload heart failure. *Circulation* 105: 236–243, 2002.
23. **Guo Y, Stein AB, Wu WJ, Zhu X, Tan W, Li Q, Bolli R.** Late preconditioning induced ny NO donors, adenosine A_1 receptor agonists, and δ_1-opioid receptor agonists is mediated by iNOS. *Am J Physiol Heart Circ Physiol* 289: H2251–H2257, 2005.
24. **Haywood GA, Tsao PS, von der Leyen HE, Mann MJ, Keeling PJ, Trindade PT, Lewis NP, Byrne CD, Rickenbacher PR, Bishopric NH, Cooke JP, McKenna WJ, Fowler MB.** Expression of inducible nitric oxide synthase in human heart failure. *Circulation* 93: 1087–1094, 1996.
25. **Heger J, Gödecke A, Flögel U, Merx MW, Molojavyi A, Kühn-Velten WN, Schrader J.** Cardiac-specific overexpression of inducible nitric oxide synthase does not result in severe cardiac dysfunction. *Circ Res* 90: 93–99, 2002.
26. **Heinzel FR, Gres P, Boengler K, Duschin A, Konietzka I, Rassaf T, Snedovskaya J, Meyer S, Skyschally A, Kelm M, Heusch G, Schulz R.** Inducible nitric oxide synthase expression and cardiomyocyte dysfunction during sustained moderate ischemia in pigs. *Circ Res* 103: 1120–1127, 2008.
27. **Hendgen-Cotta U, Grau M, Rassaf T, Gharini P, Kelm M, Kleinbongard P.** Reductive gas-phase chemiluminescence and flow injection analysis for measurement of the nitric oxide pool in biological matrices. *Methods Enzymol* 441: 295–315, 2008.
28. **Heusch G, Neumann T.** Calcium responsiveness in canine pacing-induced heart failure. *J Mol Cell Cardiol* 30: 1605–1613, 1998.
29. **Heusch G, Post H, Michel MC, Kelm M, Schulz R.** Endogenous nitric oxide and myocardial adaptation to ischemia. *Circ Res* 87: 146–152, 2000.
30. **Jaffrey SR, Erdjument-Bromage H, Ferris CD, Tempst P, Snyder SH.** Protein *S*-nitrosylation: a physiological signal for neuronal nitric oxide. *Nat Cell Biol* 3: 193–197, 2001.
31. **Jensen BC, Swigart PM, Simpson PC.** Ten commercial antibodies for alpha-1-adrenergic receptor subtypes are nonspecific. *Naunyn Schmiedebergs Arch Pharmacol* 379: 409–412, 2009.
32. **Kelm M, Schäfer S, Dahmann R, Dolu B, Perings S, Decking UK, Schrader J, Strauer BE.** Nitric oxide induced contractile dysfunction is related to a reduction in myocardial energy generation. *Cardiovasc Res* 36: 185–194, 1997.
33. **Laude K, Favre J, Thuillez C, Richard V.** NO produced by endothelial NO synthase is a mediator of delayed preconditioning-induced endothelial protection. *Am J Physiol Heart Circ Physiol* 284: H2053–H2060, 2003.
34. **Lehnart SE, Maier LS, Hasenfuss G.** Abnormalities of calcium metabolism and myocardial contractility depression in the failing heart. *Heart Fail Rev* 14: 213–224, 2009.
35. **LeWinter MM.** Functional consequences of sarcomeric protein abnormalities in failing myocardium. *Heart Fail Rev* 10: 249–257, 2005.
36. **Liang CS, Delehanty JD.** Increasing post-myocardial infarction heart failure incidence in elderly patients a call for action. *J Am Coll Cardiol* 53: 21–23, 2009.
37. **Liao X, Liu JM, Du L, Tang A, Shang Y, Wang SQ, Chen LY, Chen Q.** Nitric oxide signaling in stretch-induced apoptosis of neonatal rat cardiomyocytes. *FASEB J* 20: E1196–E1204, 2006.
38. **Liscovsky MV, Ranocchia RP, Gorlino CV, Alignani DO, Moron G, Maletto BA, Pistoresi-Palencia MC.** Interferon-gamma priming is involved in the activation of arginase by oligodeoxinucleotides containing CpG motifs in murine macrophages. *Immunology* 128: e159–e169, 2009.
39. **Little WC.** Hypertension, heart failure, and ejection fraction. *Circulation* 118: 2223–2224, 2008.
40. **Lloyd-Jones DM, Larson MG, Leip EP, Beiser A, D'Agostino RB, Kannel WB, Murabito JM, Vasan RS, Benjamin EJ, Levy D; Framingham Heart Study.** Lifetime risk for developing congestive heart failure: the Framingham Heart Study. *Circulation* 106: 3068–3072, 2002.
41. **Maekawa Y, Ouzounian M, Opavsky MA, Liu PP.** Connecting the missing link between dilated cardiomyopathy and viral myocarditis: virus, cytoskeleton, and innate immunity. *Circulation* 115: 5–8, 2007.
42. **Masaki H, Imaizumi T, Ando S, Hirooka Y, Harada S, Momohara M, Nagano M, Takeshita A.** Production of chronic congestive heart failure by rapid ventricular pacing in the rabbit. *Cardiovasc Res* 27: 828–831, 1993.
43. **Moe GW, Armstrong P.** Pacing-induced heart failure: a model to study the mechanism of disease progression and novel therapy in heart failure. *Cardiovasc Res* 42: 591–599, 1999.
44. **Mungrue IN, Gros R, You X, Pirani A, Azad A, Csont T, Schulz R, Butany J, Stewart DJ, Husain M.** Cardiomyocyte overexpression of iNOS in mice results in peroxynitrite generation, heart block, and sudden death. *J Clin Invest* 109: 735–743, 2002.
45. **Nerheim P, Birger-Botkin S, Piracha L, Olshansky B.** Heart failure and sudden death in patients with tachycardia-induced cardiomyopathy and recurrent tachycardia. *Circulation* 110: 247–252, 2004.
46. **Neumann T, Biermann J, Erbel R, Neumann A, Wasem J, Ertl G, Dietz R.** Heart failure: the commonest reason for hospital admission in Germany: medical and economic perspectives. *Dtsch Arztebl Int* 106: 269–275, 2009.
47. **Neumann T, Heusch G.** Myocardial, skeletal muscle, and renal blood flow during exercise in conscious dogs with heart failure. *Am J Physiol Heart Circ Physiol* 273: H2452–H2457, 1997.
48. **Neumann T, Ravens U, Heusch G.** Characterization of excitation-contraction coupling in conscious dogs with pacing-induced heart failure. *Cardiovasc Res* 37: 456–466, 1998.
49. **Otani H.** The role of nitric oxide in myocardial repair and remodeling. *Antioxid Redox Signal* 11: 1913–1928, 2009.
50. **Post H, Schulz R, Gres P, Heusch G.** No involvement of nitric oxide in the limitation of β-adrenergic inotropic responsiveness during ischemia. *Am J Physiol Heart Circ Physiol* 281: H2392–H2397, 2001.
51. **Pullamsetti SS, Maring D, Ghofrani HA, Mayer K, Weissmann N, Rosengarten B, Lehner M, Schudt C, Boer R, Grimminger F, Seeger W, Schermuly RT.** Effect of nitric oxide synthase (NOS) inhibition on macro- and microcirculation in a model of rat endotoxic shock. *Thromb Haemost* 95: 720–727, 2006.
52. **Rastaldo R, Pagliaro P, Cappello S, Penna C, Mancardi D, Westerhof N, Losano G.** Nitric oxide and cardiac function. *Life Sci* 81: 779–793, 2007.
53. **Razavi HM, Hamilton JA, Feng Q.** Modulation of apoptosis by nitric oxide: implications in myocardial ischemia and heart failure. *Pharmacol Ther* 106: 147–162, 2005.
54. **Rosengarten B, Wolff S, Klatt S, Schermuly RT.** Effects of inducible nitric oxide synthase inhibition or norepinephrine on the neurovascular coupling in an endotoxic rat shock model. *Crit Care* 13: R139, 2009.
55. **Schulz R, Aker S, Belosjorow S, Konietzka I, Rauen U, Heusch G.** Stress kinase phosphorylation is increased in pacing-induced heart failure in rabbits. *Am J Physiol Heart Circ Physiol* 285: H2084–H2090, 2003.
56. **Schulz R, Rassaf T, Massion PB, Kelm M, Balligand JL.** Recent advances in the understanding of the role of nitric oxide in cardiovascular homeostasis. *Pharmacol Ther* 108: 225–256, 2005.
57. **Steppan J, Ryoo S, Schuleri KH, Gregg C, Hasan RK, White AR, Bugaj LJ, Khan M, Santhanam L, Nyhan D, Shoukas AA, Hare JM, Berkowitz DE.** Arginase modulates myocardial contractility by a nitric oxide synthase 1-dependent mechanism. *Proc Natl Acad Sci USA* 103: 4759–4764, 2006.
58. **Vejlstrup NG, Bouloumie A, Boesgaard S, Andersen CB, Nielsen-Kudsk JE, Mortensen SA, Kent JD, Harrison DG, Busse R, Aldershvile J.** Inducible nitric oxide synthase (iNOS) in the human heart: expression and localization in congestive heart failure. *J Mol Cell Cardiol* 30: 1215–1223, 1998.
59. **Wang WW, Jenkinson CP, Griscavage JM, Kern RM, Arabolos NS, Byrns RE, Cederbaum SD, Ignarro LJ.** Co-induction of arginase and nitric oxide synthase in murine macrophages activated by lipopolysaccharide. *Biochem Biophys Res Commun* 210: 1009–1016, 1995.
60. **Wells SM, Holian A.** Asymmetric dimethylarginine induces oxidative and nitrosative stress in murine lung epithelial cells. *Am J Respir Cell Mol Biol* 36: 520–528, 2007.
61. **White AR, Ryoo S, Li D, Champion HC, Steppan J, Wang D, Nyhan D, Shoukas AA, Hare JM, Berkowitz DE.** Knockdown of arginase I

Downloaded from ajpheart.physiology.org on April 9, 2012

restores NO signaling in the vasculature of old rats. *Hypertension* 47: 245–251, 2006.
62. **Wunderlich C, Flögel U, Gödecke A, Heger J, Schrader J.** Acute inhibition of myoglobin impairs contractility and energy state of iNOS-overexpressing hearts. *Circ Res* 92: 1352–1358, 2003.
63. **Zhang C, Hein TW, Wang W, Miller MW, Fossum TW, McDonald MM, Humphrey JD, Kuo L.** Upregulation of vascular arginase in hypertension decreases nitric oxide-mediated dilation of coronary arterioles. *Hypertension* 44: 935–943, 2004.
64. **Zhang P, Xu X, Hu X, van Deel ED, Zhu G, Chen Y.** Inducible nitric oxide synthase deficiency protects the heart from systolic overload-induced ventricular hypertrophy and congestive heart failure. *Circ Res* 100: 1089–1098, 2007.
65. **Ziolo MT, Katoh H, Bers DM.** Expression of inducible nitric oxide synthase depresses β-adrenergic-stimulated calcium release from the sarcoplasmic reticulum in intact ventricular myocytes. *Circulation* 104: 2961–2966, 2001.
66. **Zunic G, Supic G, Magic Z, Draskovic B, Vasiljevska M.** Increased nitric oxide formation followed by increased arginase activity induces relative lack of arginine at the wound site and alters whole nutritional status in rats almost within the early healing period. *Nitric Oxide* 20: 253–258, 2009.

Downloaded from ajpheart.physiology.org on April 9, 2012